

# **Coral and symbiont adaptations to the deep reef preclude survival during local heat stress**

Giulia M. Marchioro<sup>1,2\*</sup>, Linn Yttrelid<sup>1,3</sup>, Chloe Stevenne<sup>1</sup>, Helena E. Silberhumer<sup>1,3</sup>, Michael Schagerl<sup>2,3</sup>, Luise Kruckenhauser<sup>2,4</sup>, Gerhard J. Herndl<sup>2,3</sup>, Pim Bongaerts<sup>5,6</sup>, Jennifer Hoey<sup>5</sup>, Igor Adameyko<sup>7,8</sup>, Pedro R. Frade<sup>1,2,6</sup>

<sup>1</sup> Zoological Department III, Natural History Museum Vienna, Vienna, Austria

<sup>2</sup> Vienna Doctoral School of Ecology and Evolution (VDSEE), University of Vienna, Vienna, Austria

<sup>3</sup> Department of Functional and Evolutionary Ecology, University of Vienna, Vienna, Austria

<sup>4</sup> Central Research Laboratories, Natural History Museum Vienna, Vienna, Austria

<sup>5</sup> California Academy of Sciences, San Francisco, USA

<sup>6</sup> CARMABI Foundation, Piscaderabaai, Willemstad, Curaçao

<sup>7</sup> Department of Molecular Neurosciences, Center for Brain Research, Medical University Vienna, Vienna, Austria

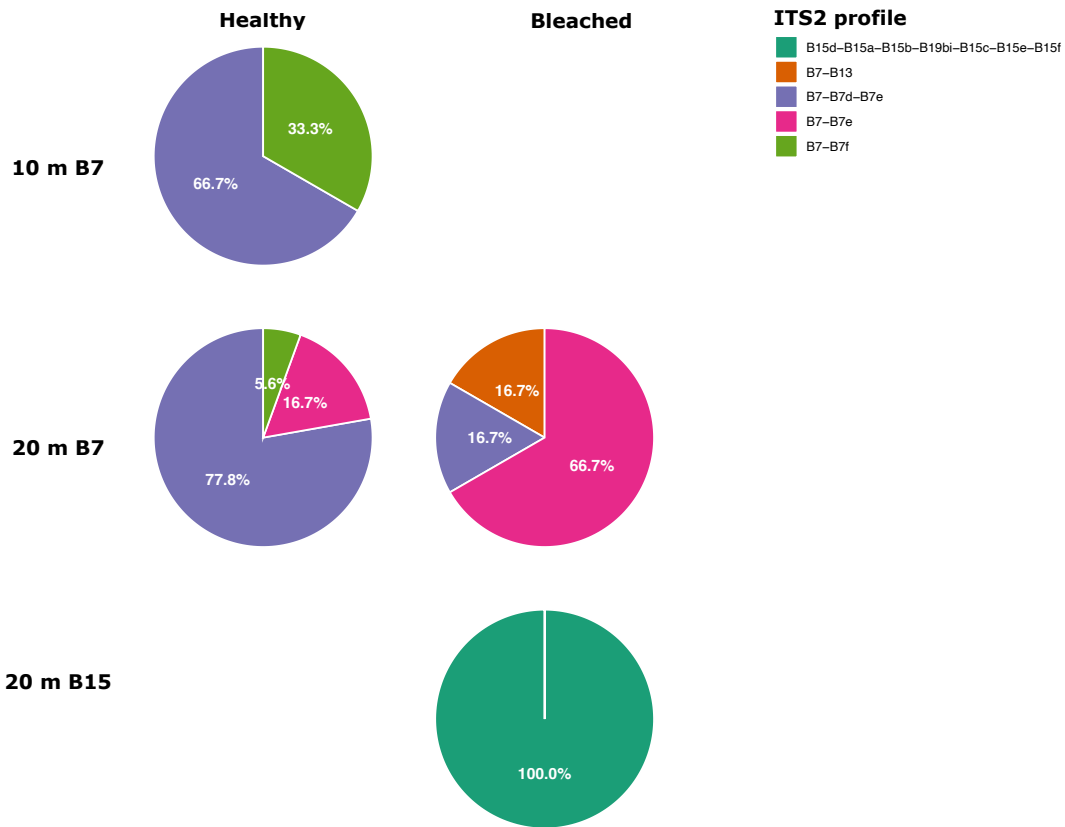
<sup>8</sup> Department of Physiology and Pharmacology, Karolinska Institute, Stockholm, Sweden

\* Correspondence:

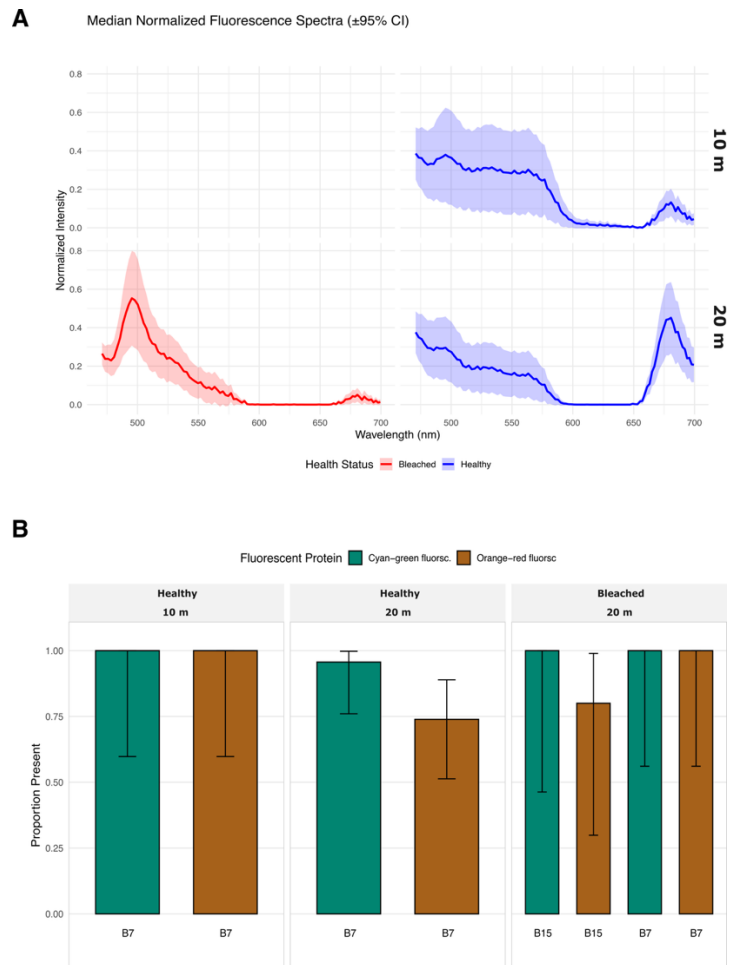
Giulia M. Marchioro

giulia.marchioro@univie.ac.at

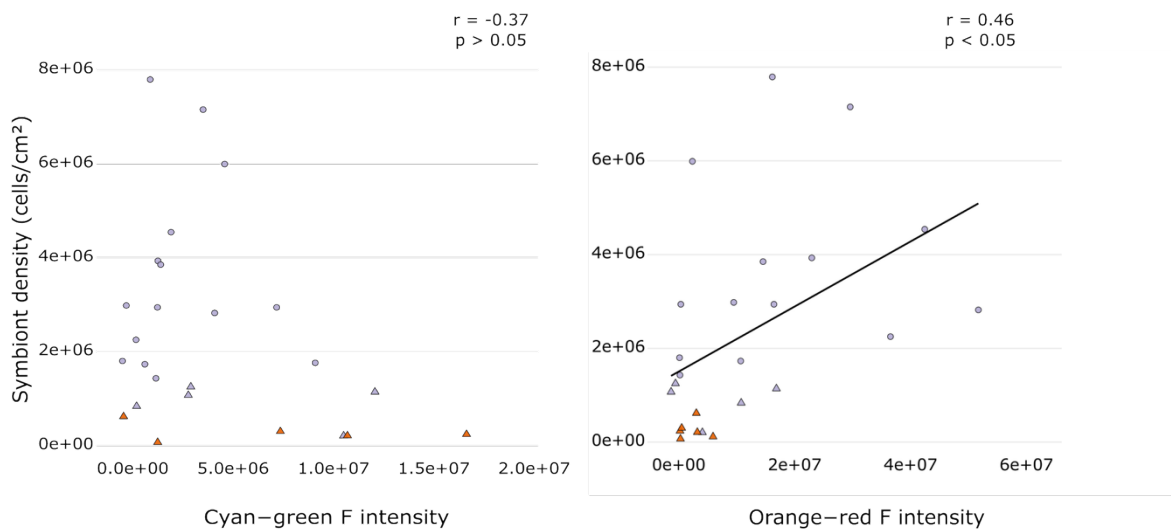
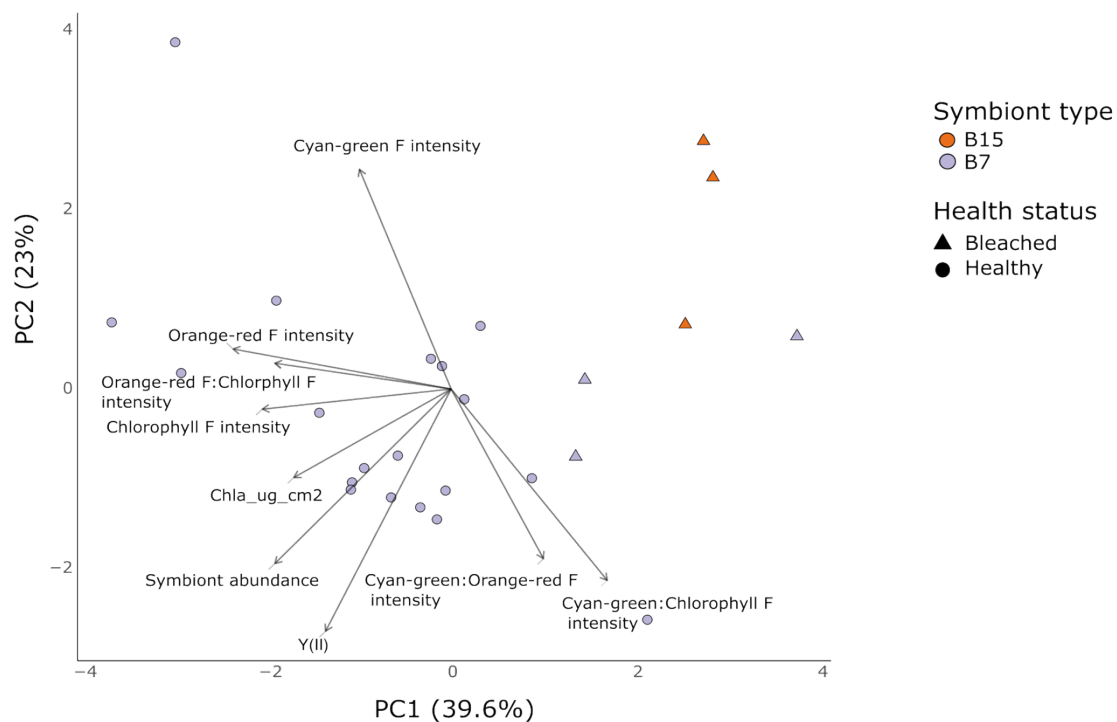
## **Supplementary Figures**



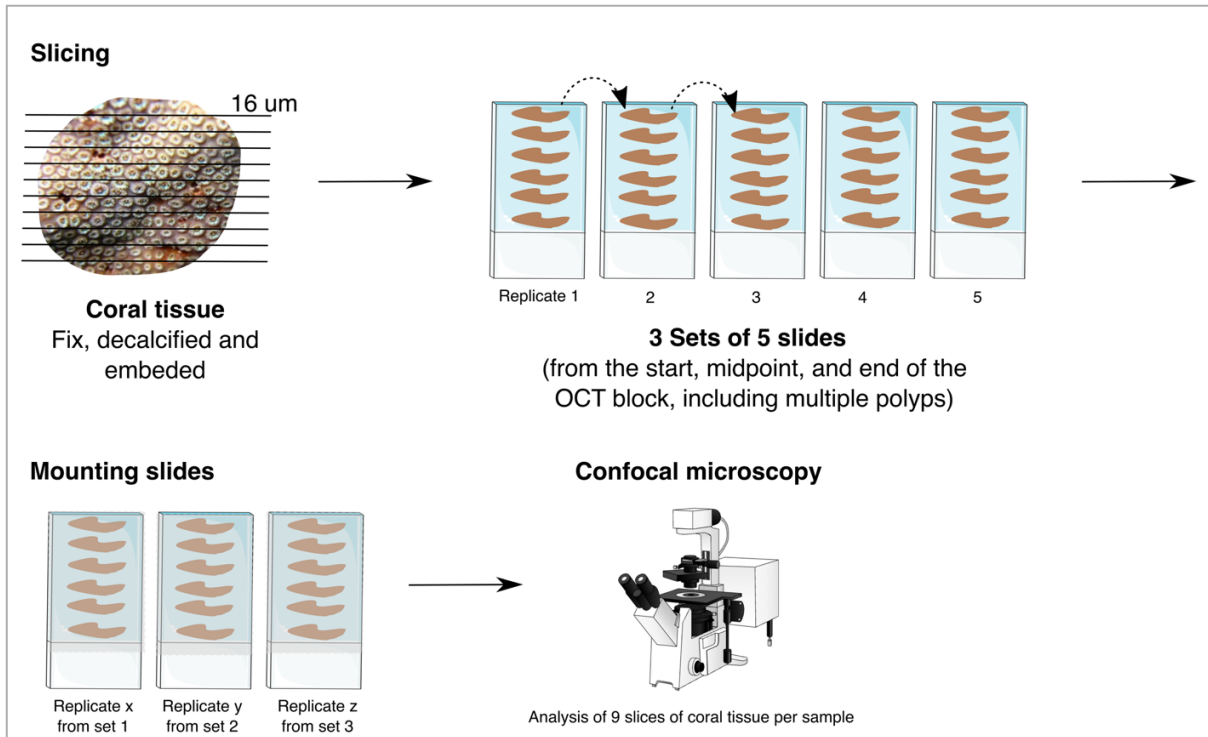
**Supplementary Figure 1. Symbiodiniaceae composition associated with *Madracis pharensis*.** Pie charts show the proportion of colonies hosting each Symbiodiniaceae type across depth and health-status categories. Colors indicate symbiont types, and percentages denote the relative frequency of colonies associated with each type. Symbiont community composition varied among categories, with some groups dominated by a single Symbiodiniaceae type and others exhibiting a more heterogeneous assemblage.



**Supplementary Figure 2. Spectral information measured in the field and prevalence of host fluorescent protein signals across depth, health status, and symbiont genotype in *Madracis pharensis*** (A) Emission spectra curves measured in the field with a spectrophotometer attached to the Diving-PAM. The spectra for the 10 m depth for healthy colonies show a large emission range present in the cyan, green, and red parts of the light spectrum (480–580 nm), with a peak in the far-red around 680 nm from the symbionts' chlorophyll. At the 20 m, a similar shape of the spectral curve is observed for healthy colonies. For bleached colonies, a more prominent peak is observed in the cyan-green range (~500 nm), with a very small peak in the chlorophyll range; (B) The bars show the proportion of colonies exhibiting detectable cyan-green and orange-red fluorescence in healthy colonies at the 10 and 20 m depths, as well as in bleached colonies at the 20 m depth. The error bars represent 95% binomial confidence intervals, and the symbiont type is represented below the bars.



**Supplementary Figure 3. Multivariate relationships between host fluorescence and symbiont physiological traits in *Madracis pharensis*.** (A) Principal Component Analysis (PCA) of coral symbiont–host physiological traits. PC1 explained 39.6% of the total variation, with the largest contributions from chlorophyll fluorescence intensity (0.510), orange–red fluorescence intensity (0.439), and their ratio (orange–red:chlorophyll, 0.377). PC2 explained 23% of the variation, driven primarily by symbiont cell density (0.456), chlorophyll-a per surface area (0.485), and photochemical efficiency of PSII (0.422); (B) Relationship between symbiont cell density and cyan–green fluorescence intensity, showing no significant correlation ( $r = -0.37$ ,  $p > 0.05$ ); (C) Positive correlation between symbiont cell density and orange–red fluorescence intensity ( $r = 0.46$ ,  $p < 0.05$ ).



**Supplementary Figure 4. Schematic overview of coral sectioning strategy and workflow.** Coral tissue was fixed, decalcified, and embedded in OCT before being cryosectioned at 16  $\mu\text{m}$  thickness. For each sample, three sets of five replicates with slices of coral tissue were collected from the beginning (1<sup>st</sup> set), midpoint (2<sup>nd</sup> set), and end (3<sup>rd</sup> set) of the OCT block, including parts of multiple polyps. From each set, one slide was selected and mounted, resulting in three mounted slides with 18 tissue slices per sample. Confocal microscopy was performed with a total of nine tissue sections analyzed per sample to capture within-sample spatial variability.